BOLETÍN DE LA SOCIEDAD ESPAÑOLA DE CERÁMICA Y VIDRIO 59 (2020) 176–184

BOLETIN DE LA SOCIEDAD ESPAÑOLA DE
Cerámica y Vidrio
www.elsevier.es/bsecv

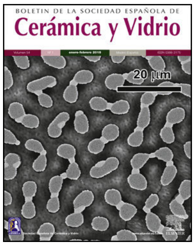

Effect of the substitution of Co^{2+} by Mg^{2+} on the color of the $CoCr_2O_4$ ceramic pigment synthesized by solution combustion

E. Chavarriaga[a,*], *A. Lopera*[b], *C. Bergmann*[c], *J. Alarcón*[d]

[a] *Departamento de Ciencias Básicas, Universidad Católica Luis Amigó, Transversal 51A # 67B 90, Medellín 050034, Colombia*
[b] *Grupo GICEI, Institución Universitaria Pascual Bravo, Calle 73 No. 73A-226, Medellín 050034, Colombia*
[c] *Laboratory of Ceramic Materials (LACER), Department of Materials Engineering, Federal University of Rio Grande do Sul (UFRGS), Osvaldo Aranha 99, Porto Alegre, RS 90035-190, Brazil*
[d] *University of Valencia, Department of Inorganic Chemistry, Calle Doctor Moliner 50, 46100 Burjasot, Valencia, Spain*

ARTICLE INFO

Article history:
Received 28 June 2019
Accepted 4 November 2019
Available online 21 November 2019

Keywords:
Solution combustion
Ceramic pigments
Spinel
Chromites
Color

ABSTRACT

This research presents the effect on the color of the green ceramic pigment $CoCr_2O_4$ when Co^{2+} was replaced by Mg^{2+}. The objective is to reduce the concentration of cobalt in the pigments, which is considered an expensive and toxic raw material. The pigments were synthesized by solution combustion in one-step. The X-ray Diffraction (XRD) and Fourier Transform Infrared Spectroscopy (FTIR) of the as-prepared powders showed that the spinel structure was obtained during the combustion reaction. The microstructure of the pigments was observed by Scanning Electron Microscopy (SEM) and the powders are porous due to the gases formed during the reaction. Finally, the color change of the powders was evidenced by UV–vis–NIR Diffuse Reflectance Spectroscopy (DRS) and calculation of CIEL*a*b* chromatic coordinates. The largest color change ΔE^*_{ab} of 9.8 was between $CoCr_2O_4$ and $MgCr_2O_4$ as a result of the absence of electronic transitions in Mg^{2+}. The results of thermal stability of the green pigments using a commercial frit showed that they could be used in ceramic decoration at 1050 °C.

Efecto de la sustitución de Co^{2+} por Mg^{2+} en el color del pigmento cerámico $CoCr_2O_4$ sintetizado por combustión en solución

Palabras clave:
Combustión en solución
Pigmentos cerámicos
Espinela
Cromitas
Color

RESUMEN

Esta investigación presenta el efecto en el color del pigmento cerámico verde $CoCr_2O_4$ cuando el Co^{2+} se sustituyó por Mg^{2+}. El objetivo es disminuir la concentración del cobalto en los pigmentos, el cual se considera una materia prima costosa y tóxica. Los pigmentos se sintetizaron en una etapa por combustión en solución. Los patrones de difracción de rayos X (DRX) y la espectroscopía de infrarrojo (IR) de los polvos mostraron la obtención de la estructura espinela durante la reacción de combustión. La microestructura de los pigmentos

---

[*] *Corresponding author.*
E-mail address: edgarchavarrigami@amigo.edu.co (E. Chavarriaga).

https://doi.org/10.1016/j.bsecv.2019.11.001

se observó por microscopía electrónica de barrido (MEB) y los polvos son porosos debido a los gases formados durante la reacción. Finalmente, el cambio de color se evidenció por espectroscopía de reflectancia difusa UV-Vis y cálculo de las coordenadas cromáticas CIEL*a*b*. El mayor cambio de color ΔE^*_{ab} de 9.8 fue entre $CoCr_2O_4$ y $MgCr_2O_4$ como consecuencia de la ausencia de transiciones electrónicas en el Mg^{2+}. Los resultados de estabilidad térmica de los pigmentos verdes usando una frita comercial mostraron que podrían ser usados en decoración cerámica a 1050 °C.

Introduction

Ceramic pigments are inorganic compounds that have high thermal and chemical stability to attack of molten glass and are used in ceramic decoration [1,2], classified in category A by Color Pigments Manufactures Association (CPMA) [3]. Spinels with general formula AB_2O_4 are a large family of inorganic compounds that have been used as magnetic materials [4], ceramic pigments [5], anode materials for lithium-ion batteries [6], catalytic materials [7]. Chromites are members of this family which have been studied in detail where $CoCr_2O_4$ and $MgCr_2O_4$ are two compositions of great interest due to their thermal stability. Cobalt chromite, $CoCr_2O_4$, has the normal spinel structure where $Co^{2+}(3d^7)$ divalent cations are in tetrahedral oxygen coordination, while $Cr^{3+}(3d^5)$ trivalent cations occupy the octahedral sites [4] with interest as ceramic pigment [8] and catalyst [9]. In recent years, the ceramic industry has been interested in using pigments with low concentration of cobalt [10], but the new compositions have good colorimetric properties among these as is the color change when a structure is diluted with a cation considered non-toxic and cheap as is the magnesium. Moreover, Magnesium chromite, $MgCr_2O_4$, also has the normal spinel structure with the $Mg^{2+}(2p^6)$ divalent cations occupy the tetrahedral sites and $Cr^{3+}(3d^5)$ trivalent cations occupy the octahedral sites [11], which is very used as a refractory material in the cement and steel industries. Therefore, it is interesting to explore the formation of a substitutional solid solution between these spinel structures to study the effect on the color when there is a substitution between Co^{2+} and Mg^{2+}.

$CoCr_2O_4$ has been synthesized by various methods such as hydrothermal synthesis [12], coprecipitation technique [13], flame spray pyrolysis [8] and solution combustion [14], among others. On the other hand, $MgCr_2O_4$ has been synthesized by polyvinyl alcohol solution using microwave [15], sol–gel route [16] and solution combustion [11], among others. These different routes of synthesis show the importance of producing these spinels.

The process of solution combustion synthesis (SCS) was discovered in India when aluminum nitrate and urea were heated up to their ignition temperature obtaining alumina in a single step [17], from then until now, the method has been used to obtain simple and complex oxides [18–21] with different properties, such as: superparamagnetism on $ZnFe_2O_4$ [22], electrical properties of calcium phosphates [23], optical properties of green spinel of $ZnCr_2O_4$ [24], and TiO_2:Pt for photocatalytic application [25]. SCS employs a self-sustaining exothermic reaction of oxidation-reduction between a fuel and an oxidant that allows obtaining high temperatures in short reaction times with a simple experimental assembly [26]. The fuel is one the most important parameters of the combustion reaction because plays an important role in controlling the temperature of reaction and therefore to obtain the phase in one-step. Urea, citric acid, and glycine are the fuels most used in the synthesis of chromites, therefore, it is interesting to use other alternative fuels with the high aim to obtain chromites in one step.

In the present paper, we report the preparation of ceramic pigments of $Co_{1-x}Mg_xCr_2O_4$ ($x = 0.0$, 0.2, 0.5, 0.7 and 1.0) for the first time a single-step using 6-aminohexanoic acid as an alternative fuel to traditional and study the effect of the substitution of Co^{2+} by Mg^{2+} on the color of $CoCr_2O_4$.

Experimental procedure

Synthesis of ceramic pigments

The ceramic pigments $Co_{1-x}Mg_xCr_2O_4$ ($x = 0.0$, 0.2, 0.5, 0.8 and 1.0) with spinel structures were synthesized by gel-combustion in a single-step using 6-aminohexanoic acid ($H_2N(CH_2)_5CO_2H$, Sigma–Aldrich, 98.5% of purity) as fuel while Chromium (III) nitrate nonahydrate ($Cr(NO_3)_3{\cdot}9H_2O$, Panreac, 98% of purity), Cobalt (II) nitrate hexahydrate ($Co(NO_3)_2{\cdot}6H_2O$, Panreac, 98% of purity), and Magnesium nitrate hexahydrate ($Mg(NO_3)_2{\cdot}6H_2O$, Aldrich, 98% of purity) are used as oxidants. The stoichiometric equation (1) of the combustion reaction in the synthesis of $CoCr_2O_4$ and $MgCr_2O_4$ is as follows:

$$M(NO_3)_2\cdot 6H_2O + 2Cr(NO_3)_3\cdot 9H_2O + 1.21C_6H_{13}NO_2 \rightarrow MCr_2O_4 + 7.26CO_{2(g)} + 4.6N_2 + 31.9H_2O \quad (1)$$

where M can be Co^{2+} or Mg^{2+}.

For obtaining 2 g of $CoCr_2O_4$. First, stoichiometric amounts of $Co(NO_3)_2{\cdot}6H_2O$ and $Cr(NO_3)_3{\cdot}9H_2O$ were taken in a glass beaker of 1000 mL and dissolved in deionized water. Then, 1.21 mole of the fuel 6-aminohexanoic acid was added to the above solution and dissolved with magnetic stirring. Afterward, the solution was slowly evaporated at 90 °C until a gel was formed. Finally, the gel was slowly heated until a reaction with flame and with gases was completed in less of 60 s. Similarly, the previous procedure was also used for the spinel structures of $Co_{0.8}Mg_{0.2}Cr_2O_4$, $Co_{0.5}Mg_{0.5}Cr_2O_4$, $Co_{0.2}Mg_{0.8}Cr_2O_4$, and $MgCr_2O_4$.

Fig. 1 – Digital images of the combustion reactions: (a) $CoCr_2O_4$, (b) $Co_{0.8}Mg_{0.2}Cr_2O_4$, (c) $Co_{0.5}Mg_{0.5}Cr_2O_4$, (d) $Co_{0.2}Mg_{0.8}Cr_2O_4$, (e) $MgCr_2O_4$.

Characterization

Crystalline structure was determined by X-ray diffraction (XRD) with a diffractometer (Model D8Controller, Bruker) equipped with a graphite monochromator using Cu K_α radiation ($\lambda = 1.54184$ Å), between 10° and 70° (2θ). The experiments were run with 1 and 6 mm divergence and antiscattering slits, respectively, with a step size of 0.02° (2θ) and an accumulated counting time of 0.2 s.

Fourier transform infrared spectrometer (FTIR, Agilent Cary 630) with attenuated total reflection (ATR) was used between 400 cm^{-1} and 4000 cm^{-1}. On the other hand, the microstructure of the as-prepared powders was analyzed by Field Emission Scanning Electron Microscopy FESEM at 20 kV (Model S-4100, Hitachi Ltd., Tokyo, Japan). The optical properties of the inorganic pigments were studied using a Jasco V-670 UV-Vis-NIR spectrophotometer with diffuse reflectance and measurement range between 200 and 1800 nm with UV–vis bandwidth of 5 nm and NIR bandwidth of 20 nm, scan speed of 400 nm/min with light source of deuterium arc lamp and Tungsten Halogen Lamp with change of source at 340 nm and change of grating at 340 nm. The color coordinates of the pigments were obtained in CIE 1976 L^*,a^*,b^* color space using the CIE standard illuminant D65 and the CIE Standard observer 10°, where L^* coordinate represents darkness (0) and brightness (100), while the a^* (red (+)–green (−) axis) and b^* (yellow(+)–blue (−)) using the ASTM E308 [27]. The color difference of the powders was calculated using Eq. (2) for chroma C^*_{ab}, Eq. (3) for hue h_{ab}, and Eq. (4) for the color difference which is defined in the standard practice for calculating of color differences D2244 [28].

CIE 1976 chroma:

$$C^*ab = \left[(a^*)^2 + (b^*)^2\right]^{1/2} \tag{2}$$

CIE 1976 hue angles:

$$\Delta H^*ab = s\left[2\left(C^*_{ab,B}C^*_{ab,standard} - a^*_B a^*_{standard} - b^*_B b^*_{standard}\right)\right]^{0.5} \tag{3}$$

where

if $a^*_{standard}b^*_B > a^*_B b^*_{standard}$ then
s = 1
else
s = −1

$$\Delta E_{ab} = \left[\Delta L^{*2} + \Delta C^{*2} + \Delta H^{*2}\right]^{0.5} \tag{4}$$

Table 1 – Thermodynamic data.

Compound	ΔH_f^0 (kJ mol^{-1})	C_p (J mol^{-1} K^{-1})	Source
$Cr(NO_3)_3{*}9H_2O$	−3631.63	–	[29]
$Co(NO_3)_2{*}6H_2O$	−2212.68	–	[35]
$Mg(NO_3)_2{*}6H_2O$	−2614.57	–	[36]
$C_6H_{13}NO_2$	−637.77	–	[37]
$CoCr_2O_4$	−1432.81	130.25	[38]
$MgCr_2O_4$	−1763.19	227.38	[39]
CO_2	−393.77	37.26	[35]
H_2O	−241.95	30.14	[35]
N_2	0	27.21	[35]

Results and discussion

Adiabatic temperatures for the combustion reactions on the synthesis of $CoCr_2O_4$ and $MgCr_2O_4$

Fig. 1 shows digital images of the combustion reactions of all the reactions as can be seen there is the presence of a flame permits where the least intense is for the synthesis of $MgCr_2O_4$. The heats of combustion ΔH^0 for the synthesis of $CoCr_2O_4$ and $MgCr_2O_4$ were calculated using the thermodynamic data in Table 1 which can be expressed using Eq. (5)

$$\Delta H^0 = \sum n\left(\Delta H_f^0\right)_{products} - \sum n\left(\Delta H_f^0\right)_{reactants} \tag{5}$$

where n is the number of moles and $\Delta H_f{}^0$ is the standard enthalpy of formation for the reactants and products.

The adiabatic flame temperatures were estimated using Eq. (6) where m is the number of moles of each product, T_{ad} is the adiabatic flame temperature and C_p represents the specific heat of the products.

$$Q = -\Delta H^0 = \int_{298}^{T_{ad}} \left(\sum mC_p\right)_{products} dT \tag{6}$$

In this process, the combustion reaction occurs when the precursor mixture is dehydrated into gel above the room temperature until its ignition temperature.

The heat of the reactions are $\Delta H = -1761$ kJ and $\Delta H = -1689$ kJ for $CoCr_2O_4$ and $MgCr_2O_4$, respectively, and the adiabatic flame temperatures are 1482 K and 1347 K for $CoCr_2O_4$ and $MgCr_2O_4$, respectively. These results show that the high temperature during the reactions can be sufficient for the formation of the spinel phase in a single state where the temperature of the reaction when $MgCr_2O_4$ was synthesized is lower than $CoCr_2O_4$. Recently, Chamyani et al. [29] estimated adiabatic flame temperatures of the combustion reactions in the synthesis of $CoCr_2O_4$ using different fuels, and they obtained a $T_{ad} = 1266$ K when the citric acid was used as fuel, but if the mixture of fuels citric acid and ethylenediamine was used the $T_{ad} = 1412$ K. However, in our case when the

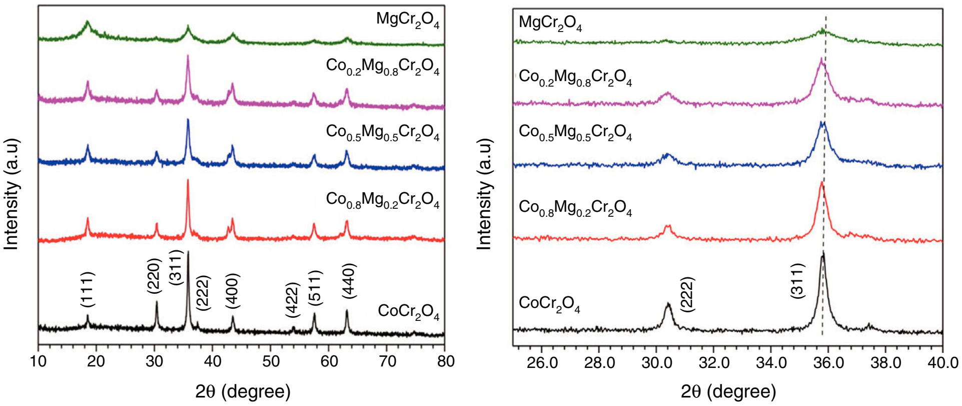

Fig. 2 – XRD patterns for the as-prepared powders.

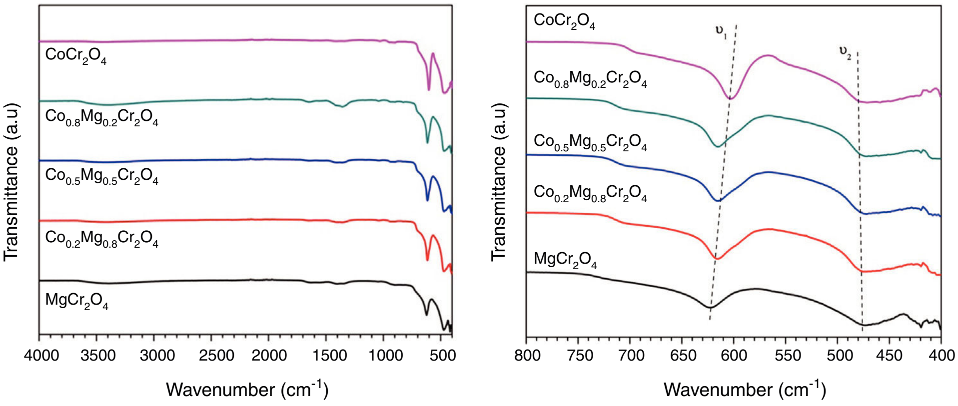

Fig. 3 – Infrared spectra for the as-prepared powders.

Table 2 – Absorption vibration modes of as-prepared powders.

Compound	Absorption vibration (cm^{-1}) octahedral group	Absorption vibration (cm^{-1}) tetrahedral group
$CoCr_2O_4$	464	602
$Co_{0.8}Mg_{0.2}Cr_2O_4$	468	614
$Co_{0.5}Mg_{0.5}Cr_2O_4$	469	614
$Co_{0.2}Mg_{0.8}Cr_2O_4$	470	614
$MgCr_2O_4$	472	622

6-aminohexanoic acid as single fuel, the adiabatic flame temperature estimated is higher than the mixture of fuels used by Chamyani et al. On the other hand, De Andrade et al. [11] calculated the adiabatic flame temperature in the synthesis of $MgCr_2O_4$ using glycine and urea as fuels, $T_{ad} = 1300$ K and $T_{ad} = 1200$ K, respectively. In our case using a 6-aminohexanoic acid as single fuel, the adiabatic flame temperature is also higher than the mixture of fuel and extra-oxidant used by De Andrade et al.

X-ray diffraction patterns and IR spectra of the ceramic pigments

Fig. 2 shows the XRD patterns of the as-prepared powders with compositions $CoCr_2O_4$, $Co_{0.8}Mg_{0.2}Cr_2O_4$, $Co_{0.5}Mg_{0.5}Cr_2O_4$, $Co_{0.2}Mg_{0.8}Cr_2O_4$, and $MgCr_2O_4$. The patterns obtained confirm the formation of the cubic spinel structure with Space Group Fd3m (227) and with well-defined peaks around 18.5°, 30.4°, 35.8°, 37.4°, 43.5°, 53.9°, 57.6° and 63.2° (2θ) which are respectively ascribed to the (111), (220), (311), (222), (400), (422), (511) and (440) planes of $CoCr_2O_4$ (JCPDS 22-1084) and $MgCr_2O_4$ (JCPDS 10-0351). The intensity of the main peak (311) of the as-prepared powder decreases with the increase of the concentration of Mg this is due at the different temperatures during the combustion reaction as it was shown in the calculation of flame temperature. Therefore, in the pattern of $CoCr_2O_4$ is observed that there is a higher crystallization than $MgCr_2O_4$. It is interesting to observe the slight shift to right in the peak associated with the main plane (331) in the XRD patterns with respect to the standard, this is due to differences in ionic size,

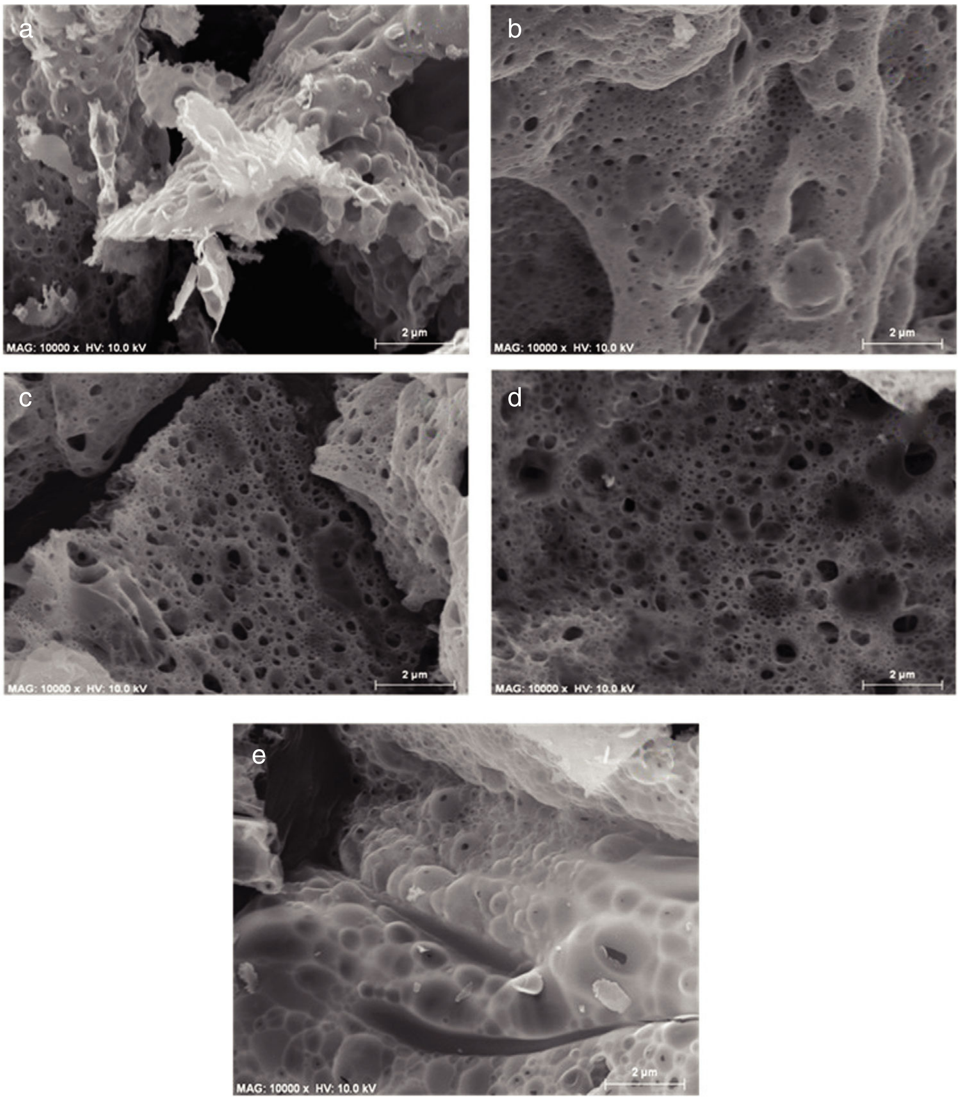

Fig. 4 – SEM micrographs for the as-prepared powders: (a) $CoCr_2O_4$, (b) $Co_{0.8}Mg_{0.2}Cr_2O_4$, (c) $Co_{0.5}Mg_{0.5}Cr_2O_4$, (d) $Co_{0.2}Mg_{0.8}Cr_2O_4$, and (e) $MgCr_2O_4$.

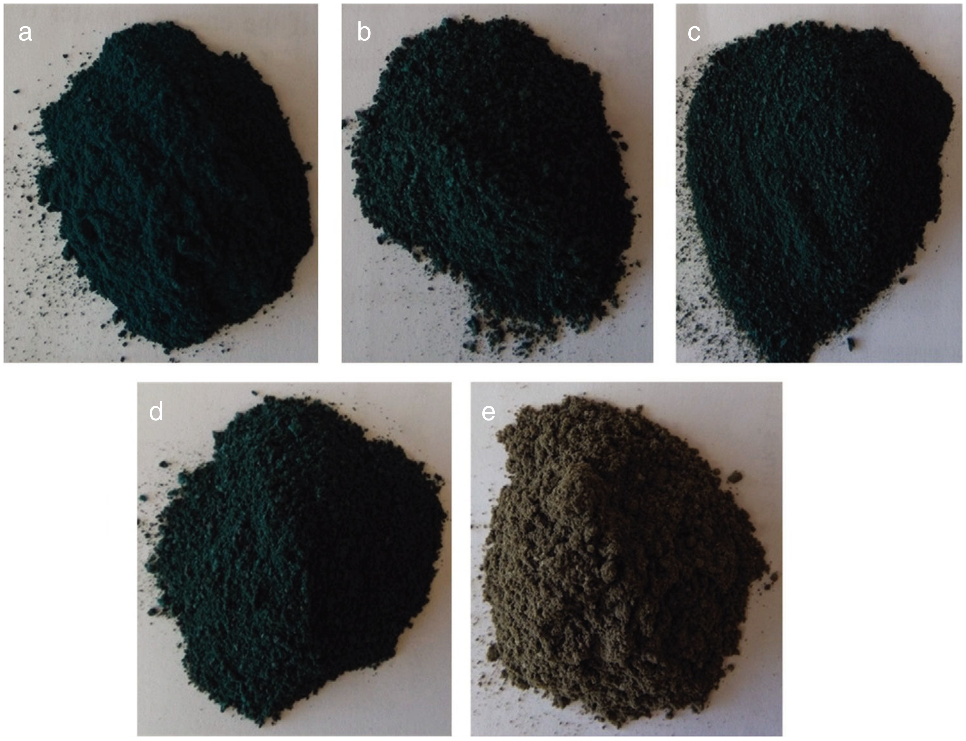

Fig. 5 – Digital images for the as-prepared powders: (a) $CoCr_2O_4$, (b) $Co_{0.8}Mg_{0.2}Cr_2O_4$, (c) $Co_{0.5}Mg_{0.5}Cr_2O_4$, (d) $Co_{0.2}Mg_{0.8}Cr_2O_4$, and (e) $MgCr_2O_4$.

The cristal radii of Co^{2+} in four coordination and High Spin is 72 pm, while for the Mg^{2+} cation in four coordination is 71 pm [30]. Using the Bragg's law, the lattice parameter was determined for $CoCr_2O_4$ and its value is 0.8314 nm, whereas for $MgCr_2O_4$ was 0.8312 nm which shows a slight variation when Co^{2+} is replaced by Mg^{2+}, this observation is in agreement with the small difference of their crystal radii. These results agree with those reported by Hu et al. [31]. Moreover, the different ionic sizes and chemical behavior of Mg^{2+} and Co^{2+} could originate different crystallization rates for each chromite. For example, Gilabert et al. [21] found that there is a huge change in the crystallinity of the spinel as one cation is substituted by another.

Fig. 3 shows the FTIR spectra of the as-prepared powders where the characteristic absorption bands of the structure are shown in Table 2. Kumar et al. [16] report the FTIR spectrum of $MgCr_2O_4$ and observed absorption bands at $\upsilon_1 = 632$ and $\upsilon_2 = 430\,cm^{-1}$ arising from the vibration absorption of octahedral for Cr–O and tetrahedral for Co-O, respectively. On the other hand, Maczka et al. [5] obtained the FTIR spectrum of $CoCr_2O_4$ and found absorption bands at $\upsilon_1 = 631$ and $\upsilon_2 = 493\,cm^{-1}$ which can be attributed to the vibration absorption of tetrahedral group CoO_4 and octahedral group CrO_6, respectively. All the observed vibrations have an increase in wavenumber when cobalt is replaced by magnesium which is due to differences in ionic sizes while the shift in band positions not is observed for the octahedral group CrO_6, this can be associated with normal spinels synthesized. Therefore, these results confirm the formation of the spinel structure.

Fig. 4 shows the SEM micrographs of the as-prepared powders and is evident the formation of porous powders, which is due to the gases released during the reaction of combustion as has occurred in other combustion syntheses [26], there is also the formation of agglomerates of primary particles with irregular shape, this is a consequence of the high temperatures during the combustions. Images of SEM show that it is not possible to find an effect on the morphology with the increase of the concentration of Mg^{2+} in the structure.

*Optical absorption and color coordinates L*a*b**

Fig. 5 shows the digital images of the as-prepared powders where is evident the change in the color in the powders between $CoCr_2O_4$ and $MgCr_2O_4$ due to the absorption of the visible light, because when Co^{2+} is present the green color is darker than with Mg^{2+}.

Fig. 6 shows the spectra of the as-prepared powders with compositions $Co_{1-x}Mg_xCr_2O_4$ ($x = 0.0$, 0.2, 0.5, 0.7 and 1.0) which have bands around 272, 345, 423, 609, 657 and 1560 nm. These spectra are very similar to the spectra of $MgCr_2O_4$ and $CoCr_2O_4$ reported in the literature [32–34]. Therefore, the band around 272 nm can be attributed to the charge-transfer transition between O^{2-} and Cr^{3+} [32–34]. Bands in the range 350–500 nm are associated to ${}^4A_{2g} \rightarrow {}^4T_{1g}$ and ${}^4A_{2g} \rightarrow {}^2T_{2g}$ transitions of the octahedral coordinated Cr^{3+} ion [32–34]. The bands around 609 and 657 nm can be assigned with ${}^4A_2({}^4F) \rightarrow {}^4T_1({}^4P)$ transitions of the Co^{2+} ion in tetrahedral coordination as well as ${}^4A_{2g} \rightarrow {}^4T_{2g}$ and ${}^4A_{2g} \rightarrow {}^2T_{1g}$ transitions

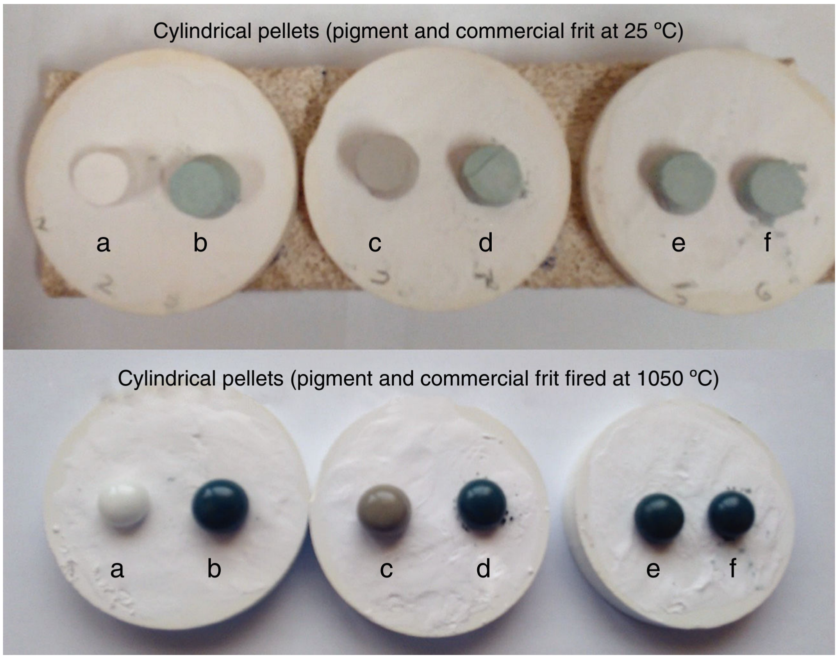

Fig. 7 – Digital images (a) frit without pigment, and frit with the pigments, (b) $CoCr_2O_4$, (c) $MgCr_2O_4$, (d) $Co_{0.8}Mg_{0.2}Cr_2O_4$, (e) $Co_{0.5}Mg_{0.5}Cr_2O_4$, and (f) $Co_{0.2}Mg_{0.8}Cr_2O_4$.

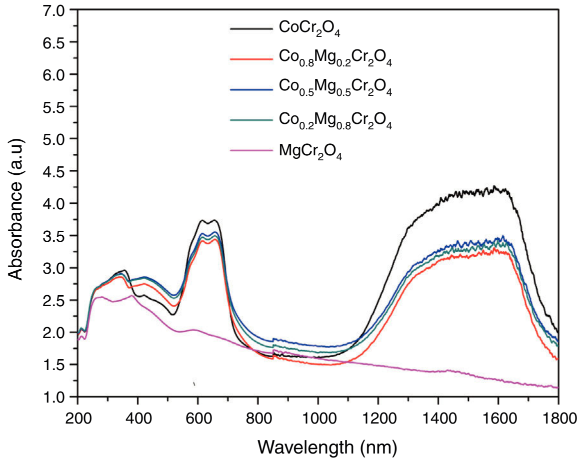

Fig. 6 – UV–vis–NIR absorbance spectra for the chromites.

of Cr^{3+} [32–34]. Finally, bands in the 1300–1620 nm range are due to $^4A_2(^4F) \rightarrow {}^4T_1(^4F)$ transitions of Co^{2+} [32–34]. Spectra of the powders are very similar, but the spectrum of $MgCr_2O_4$ is different due to the absence of the electronic transitions of Co^{2+}. Therefore, our absorption spectra show very clearly the effect of substituting the chromophore on the optical properties of the powders.

Table 3 shows the change in the color coordinates CIEL*a*b* of the as-prepared powders are green-blue where the a^* and b^* coordinates decrease when the Co^{2+} is substituted by Mg^{2+} which is due to the disappearance of electronic d-d transitions in Co^{2+}. Therefore, the chroma decreases when the substitution by Mg^{2+} increases. On the other hand, the hue shows a change of color toward a green which is due to a decrease in the blue coordinate. However, all the powders have not changed in the L^* values, which can be associated with a few influences of the morphology in the scattering of the light. The highest color change (ΔE^*_{ab}) using the as-prepared powder of $CoCr_2O_4$ as reference was observed when there is a substitution complete between Co^{2+} and Mg^{2+}. Moreover, the change in the color (ΔE^*_{ab}) for the substitutions of Mg between $x = 0.2$ and $x = 0.8$ was 3.2 which shows that the dilution of $CoCr_2O_4$ permits to obtain green pigments without a change in the color when the cobalt is in the structure.

The thermal stability of the pigments prepared by solution combustion was evaluated in a commercial frit as is shown in Fig. 7. The pigments were mixed with an industrial CaO–ZnO–SiO_2 frit (5 wt% of the pigment) and cylindrical pellets have been made and after drying the samples were fired

Table 3 – Color coordinates CIEL*a*b* for the ceramic pigments.

Compound	L^*	a^*	b^*	Chroma C^*_{ab}	ΔH_{ab}	ΔE^*_{ab}
$CoCr_2O_4$ (standard)	63.7	−13.3	−8.1	15.6		
$Co_{0.8}Mg_{0.2}Cr_2O_4$	64.3	−11.9	−5.3	13.0	−1.82	3.2
$Co_{0.5}Mg_{0.5}Cr_2O_4$	64.2	−11.3	−5.4	12.5	−1.41	3.4
$Co_{0.2}Mg_{0.8}Cr_2O_4$	64.2	−11.4	−5.2	12.5	−1.66	3.5
$MgCr_2O_4$	64.7	−6.8	−0.9	6.9	−4.26	9.8

at 1050 °C for 5 min. The heating rate up to 1050 °C has been 10 °C min^{-1}. As can be seen good thermal and chemical stability into the frit was obtained in all samples and the pigments had green color after glazing. Therefore, the pigments can be classified in the category A of CPMA which is important in the production of inorganic pigments with a lower concentration of cobalt for applications in ceramic decoration.

Conclusions

Ceramic pigments with compositions $Co_{1-x}Mg_xCr_2O_4$ ($x = 0.0$, 0.2, 0.5, 0.7 and 1.0) were synthesized by gel combustion in one-step using 6-aminohexanoic acid. The adiabatic flame temperatures are 1482 K and 1347 K for $CoCr_2O_4$ and $MgCr_2O_4$, respectively, which is important for the control of crystallization during the reaction. Moreover, the micrographs in SEM showed agglomerated particles and porosity in the powders. On the other hand, the effect of substituting Co^{2+} by Mg^{2+} change of the color on the powders with the highest color change (ΔE^*_{ab}) using the as-prepared powder of $CoCr_2O_4$ as reference was observed when there is a substitution complete between Co^{2+} and Mg^{2+}. Furthermore, these results show the possibility of using gel-combustion in the synthesis of ceramic pigments. The results of thermal stability of the green pigments using a commercial frit showed that they could be used in ceramic decoration at 1050 °C.

Acknowledgments

Authors are very grateful to Colciencias - Colombia. Project “Fellowship for National Doctorates calls 647” for Doctoral Training Award to E. A. Chavarriaga. Fellowship Jóvenes Investigadores 2017 - Universidad de Valencia, Spain.

REFERENCES

[1] G. Monros, Pigment, Ceramic, in: Ronnier Luo (Ed.), Encycl. Color Sci. Technol., Springer, 2014, pp. 1026–1040 http://www.springerreference.com/docs/html/chapterdbid/348055.html.

[2] R.A. EPPLER, Colorants for ceramics, in: Kirk-Othmer (Ed.), Encycl. Chem. Technol., John Wiley & Sons, Inc, 2013, pp. 1–17, http://dx.doi.org/10.1002/0471238961.0315121505161612.a01.pub3.

[3] CPMA Classification and Chemical Description of the Complex Inorganic Color Pigments, 4th ed., Alexandria, Dry Color Manufactures Associations, 2010.

[4] M. Akyol, İ. Adanur, A.O. Ayaş, A. Ekicibil, Magnetic field dependence of magnetic coupling in $CoCr_2O_4$ nanoparticles, Physica B: Condens. Matter. 525 (2017) 144–148, http://dx.doi.org/10.1016/j.physb.2017.09.021.

[5] M. Mączka, M. Ptak, M. Kurnatowska, J. Hanuza, Synthesis, phonon and optical properties of nanosized $CoCr_2O_4$, Mater. Chem. Phys. 138 (2013) 682–688, http://dx.doi.org/10.1016/j.matchemphys.2012.12.039.

[6] J. Li, Q. Meng, Y. Zhang, L. Peng, G. Yu, A.C. Marschilok, L. Wu, D. Su, K.J. Takeuchi, E.S. Takeuchi, Y. Zhu, E.A. Stach, Size-dependent kinetics during non-equilibrium lithiation of nano-sized zinc ferrite, Nat. Commun. (2019) 1–8, http://dx.doi.org/10.1038/s41467-018-07831-5.

[7] Z. Wang, J. Deng, Y. Liu, H. Yang, S. Xie, Z. Wu, H. Dai, Three-dimensionally ordered macroporous $CoCr_2O_4$-supported Au–Pd alloy nanoparticles: highly active catalysts for methane combustion, Catal. Today 281 (2017) 467–476, http://dx.doi.org/10.1016/j.cattod.2016.05.035.

[8] N. Betancur-Granados, O.J. Restrepo-Baena, Flame spray pyrolysis synthesis of ceramic nanopigments $CoCr_2O_4$: the effect of key variables, J. Eur. Ceram. Soc. 37 (2017) 5051–5056, http://dx.doi.org/10.1016/j.jeurceramsoc.2017.06.024.

[9] D. Fino, N. Russo, G. Saracco, V. Specchia, Catalytic removal of NO_x and diesel soot over nanostructured spinel-type oxides, J. Catal. 242 (2006) 38–47, http://dx.doi.org/10.1016/j.jcat.2006.05.023.

[10] C.G. García, S.C. Lloria, N.F. Argamasilla, M. Llusar, G. Monrós, Estudio de la capacidad fotocatalítica y refrigerante de una nueva paleta de pigmentos, Bol. Soc. Españ. Cerám. Y Vidr. 56 (2017) 166–176, http://dx.doi.org/10.1016/j.bsecv.2017.01.001.

[11] M.J. de Andrade, M.D. Lima, R. Bonadiman, C.P. Bergmann, Nanocrystalline pirochromite spinel through solution combustion synthesis, Mater. Res. Bull. 41 (2006) 2070–2079, http://dx.doi.org/10.1016/j.materresbull.2006.04.002.

[12] A. Abbasi, M. Hamadanian, M. Salavati-Niasari, M.P. Mazhari, Hydrothermal synthesis, characterization and photodegradation of organic pollutants of $CoCr_2O_4$/Ag nanostructure and thermal stability of epoxy acrylate nanocomposite, Adv. Powder Technol. 28 (2017) 2756–2765, http://dx.doi.org/10.1016/j.apt.2017.08.001.

[13] J.K. Galivarapu, D. Kumar, A. Banerjee, C. Rath, Magnetic transitions in chemically synthesized nanoparticles of $CoCr_2O_4$, IEEE Trans. Magn. 52 (2016) 1–6, http://dx.doi.org/10.1109/TMAG. 2016.2537794.

[14] J. Gilabert, M.D. Palacios, V. Sanz, S. Mestre, Solution combustion synthesis of $(Co,Ni)Cr_2O_4$ pigments: influence of initial solution concentration, Ceram. Int. 43 (2017) 10032–10040, http://dx.doi.org/10.1016/j.ceramint.2017.05.019.

[15] H. Lü, W. Ma, H. Zhao, J. Du, X. Yu, Synthesis and characterization of $MgCr_2O_4$:Co^{2+} fabricated by a microwave method, Mater. Manuf. Process. 26 (2011) 1233–1235, http://dx.doi.org/10.1080/10426914.2010.544810.

[16] V.K. Tripathi, R. Nagarajan, Rapid synthesis of mesoporous, nano-sized $MgCr_2O_4$ and its catalytic properties, J. Am. Ceram. Soc. 99 (2016) 814–818, http://dx.doi.org/10.1111/jace.14036.

[17] K. Patil, M. Hedge, T. Rattan, S. Aruna, Chemistry of nanocrystalline oxide materials, in: Combustion Synthesis, Properties and Applications, World Scientific, Singapore, 2008, http://dx.doi.org/10.1142/9789812793157_0001.

[18] F. Legorreta-garcía, L.E. Hernández-cruz, M.A. Flores-gonzález, M. Villanueva-ibá, Synthesis, characterization and thermal stability of solid solutions $Zr(Y,Fe, Mo)O_2$, Bol. Soc. Españ. Cerám. Y Vidr. 4 (2015) 119–123, http://dx.doi.org/10.1016/j.bsecv.2015.05.004.

[19] J.A. Gómez-cuaspud, E. Vera-lópez, S. Ni, Synthesis and characterization of $La_{0.8}Sr_{0.2}Ni_{(1-x)}Cr_xO_3$ ($x = 0.0$, 0.2, 0.4, 0.6, 0.8, 1.0) system by the combustion method, Bol. Soc. Españ. Cerám. Y Vidr. 56 (2017) 273–282, http://dx.doi.org/10.1016/j.bsecv.2017.05.004.

[20] D. Bovand, A. Masoud, M. Bovand, Microwave assisted solution combustion synthesis of β-tricalcium phosphate nano-powders, Bol. Soc. Españ. Cerám. Y Vidr. 57 (2018) 240–246, http://dx.doi.org/10.1016/j.bsecv.2018.05.001.

[21] J. Gilabert, M. Dolores, V. Sanz, S. Mestre, Fuel effect on solution combustion synthesis of $Co(Cr,Al)_2O_4$ pigments, Bol. Soc. Españ. Cerám. Y Vidr. 56 (2017) 215–225, http://dx.doi.org/10.1016/j.bsecv.2017.03.003.

[22] Z.A. Gilani, M.S. Shifa, H.M.N. ul Huda Khan Asghar, M.A. Khan, M.N. Anjum, M.N. Usmani, R. Ali, M.F. Warsi, New

$LiCo_{0.5}Pr_xFe_{2-x}O_4$ nanoferrites: prepared via low cost technique for high density storage application, Ceram. Int. 44 (2018) 1881–1885, http://dx.doi.org/10.1016/j.ceramint.2017.10.126.

[23] A.A. Lopera, E.A. Chavarriaga, B. Zuluaga, S. Marin, G.O. Giraldo, H.A. Estupiñan, V. Zapata, C.P. Garcia, Effect of salt concentration on the electrical and morphological properties of calcium phosphates obtained via microwave-induced combustion synthesis, Adv. Powder Technol. 28 (2017) 2787–2795, http://dx.doi.org/10.1016/j.apt.2017.08.007.

[24] E.A.C. Miranda, J.F.M. Carvajal, O.J.R. Baena, Effect of the fuels glycine, urea and citric acid on synthesis of the ceramic pigment $ZnCr_2O_4$ by solution combustion, Mater. Res. 18 (2015) 1038–1043, http://dx.doi.org/10.1590/1516-1439.019915.

[25] A.A. Lopera, E.A. Chavarriaga, H.A. Estupiñan, I.C. Valencia, C. Paucar, C.P. Garcia, Synthesis and spectroscopic characterization of nanoparticles of TiO_2 doped with Pt produced via the self-combustion route, J. Physica D: Appl. Phys. 49 (2016) 205501, http://dx.doi.org/10.1088/0022-3727/49/20/205501.

[26] B.F. Alves, Annelise, Bergmann Carlos, Novel Synthesis and Characterization of Nanostructures Materials, Berlin, 2013, http://dx.doi.org/10.1007/978-3-642-41275-2.

[27] ASTM, Standard Practice for Computing the Colors of Objects by Using the CIE System, ASTM E308-13, 2014, http://dx.doi.org/10.1520/E0308-13.2.

[28] ASTM, Standard Practice for Calculation of Color Tolerances and Color Differences from Instrumentally Measured Color Coordinates. ASTM D2244-15, 2015, http://dx.doi.org/10.1520/D2244-15.2.

[29] S. Chamyani, A. Salehirad, N. Oroujzadeh, D.S. Fateh, Effect of fuel type on structural and physicochemical properties of solution combustion synthesized $CoCr_2O_4$ ceramic pigment nanoparticles, Ceram. Int. (2018) 1–7, http://dx.doi.org/10.1016/j.ceramint.2018.01.205.

[30] R.D. Shannon, Revised effective ionic radii and systematic studies of interatomie distances in halides and chaleogenides, Acta Cryst. A, 32 (1976) 751–767, doi:10.1107/S0567739476001551.

[31] J. Hu, W. Zhao, R. Hu, G. Chang, C. Li, L. Wang, Catalytic activity of spinel oxides $MgCr_2O_4$ and $CoCr_2O_4$ for methane combustion, Mater. Res. Bull. 57 (2014) 268–273, http://dx.doi.org/10.1016/j.materresbull.2014.06.001.

[32] M. Ma, M. Ptak, M. Kurnatowska, J. Hanuza, Synthesis, phonon and optical properties of nanosized $CoCr_2O_4$ 138 (2013) 682–688, http://dx.doi.org/10.1016/j.matchemphys.2012.12.039.

[33] S.A. Eliziário, J.M. De Andrade, S.J.G. Lima, C.A. Paskocimas, L.E.B. Soledade, P. Hammer, E. Longo, A.G. Souza, I.M.G. Santos, Black and green pigments based on chromium–cobalt spinels 129 (2011) 619–624, http://dx.doi.org/10.1016/j.matchemphys.2011.05.001.

[34] A.V. Knyazev, M. Ma, E.N. Bulanov, M. Ptak, S.S. Belopolskaya, High-temperature thermal and X-ray diffraction studies, and room-temperature spectroscopic investigation of some inorganic pigments, Dyes Pigments 91 (2011) 286–293, http://dx.doi.org/10.1016/j.dyepig.2011.05.018.

[35] A.B. Salunkhe, V.M. Khot, M.R. Phadatare, S.H. Pawar, Combustion synthesis of cobalt ferrite nanoparticles – influence of fuel to oxidizer ratio, J. Alloys Compd. 514 (2012) 91–96, http://dx.doi.org/10.1016/j.jallcom.2011.10.094.

[36] V.M. Khot, A.B. Salunkhe, M.R. Phadatare, S.H. Pawar, Formation, microstructure and magnetic properties of nanocrystalline $MgFe_2O_4$, Mater. Chem. Phys. 132 (2012) 782–787, http://dx.doi.org/10.1016/j.matchemphys.2011.12.012.

[37] I. Contineanu, L. Chivu, Ş. Perişanu, The enthalpies of combustion and formation of L-α-glutamic and 6-aminohexanoic acids, J. Therm. Anal. Calorim. 82 (2005) 3–6, http://dx.doi.org/10.1007/s10973-005-0887-z.

[38] S.E. Ziemniak, L.M. Anovitz, R.A. Castelli, W.D. Porter, Thermodynamics of Cr_2O_3, $FeCr_2O_4$, $ZnCr_2O_4$, and $CoCr_2O_4$, J. Chem. Thermodyn. 39 (2007) 1474–1492, http://dx.doi.org/10.1016/j.jct.2007.03.001.

[39] S.T.K. Lemme, H. Eill, W.A.S. Chnelle, E.B.G. Melin, The heat capacity of $MgCr_2O_4$, $FeCr_2O_4$, and Cr_2O_3 at low temperatures and derived, Am. Miner. 85 (2000) 1686–1693, http://dx.doi.org/10.1007/s00269-005-0003-8.